Spin-parity assignments in ^{15}C* by a new method: β-delayed spectroscopy for a spin-polarized nucleus

H. Miyatake,[1,*] H. Ueno,[2] Y. Yamamoto,[3] N. Aoi,[4] K. Asahi,[2,5] E. Ideguchi,[2] M. Ishihara,[2,4] H. Izumi,[3] T. Kishida,[2] T. Kubo,[2] S. Mitsuoka,[6] Y. Mizoi,[2] M. Notani,[2] H. Ogawa,[2] A. Ozawa,[2] M. Sasaki,[3] T. Shimoda,[3] T. Shirakura,[3] N. Takahashi,[3] S. Tanimoto,[3] and K. Yoneda[4]

[1]*Institute of Particle and Nuclear Studies (IPNS), High Energy Accelerator Research Organization (KEK), Ibaraki, 305-0801 Japan*

[2]*The Institute of Physical and Chemical Research (RIKEN), Saitama 351-0198, Japan*

[3]*Department of Physics, Graduate School of Science, Osaka University, Osaka 560-0043, Japan*

[4]*Department of Physics, Graduate School of Science, University of Tokyo, Tokyo 113-8654, Japan*

[5]*Department of Physics, Faculty of Science, Tokyo Institute of Technology, Tokyo 152-8550, Japan*

[6]*Japan Atomic Energy Research Institute (JAERI), Ibaraki 319-1195, Japan*

(Received 1 February 2002; revised manuscript received 31 October 2002; published 17 January 2003)

We propose a method of spin-parity assignments in decay spectroscopy. Its feasibility was tested for the β-delayed neutron decay of *spin-polarized* ^{15}B. The β-decay asymmetries were measured in coincidence with the delayed neutrons, and the AP values were evaluated for five allowed transitions leading to the excited states in ^{15}C (E_x=3.103, 4.220, 4.657, 5.866, and 6.426 MeV). The spin parities of the former three states were uniquely assigned as $1/2^-$, $5/2^-$, and $3/2^-$, respectively. These assignments are consistent with the previous assignments. Because of insufficient statistics for the 5.866-MeV state ($1/2^-$), an incorrect assignment ($3/2^-$) could not be excluded within the 1σ deviation. The spin-parity of the 6.417-MeV state is suggested to be $1/2^-$. The peak analysis with detector response in the neutron time of flight spectra enabled precise determinations of the level energies and widths. The level widths were determined for the first time. The present method is also applicable for β-delayed proton, α, and γ decays, and it can be a powerful tool for spectroscopic studies of nuclei far from the stability.

DOI: 10.1103/PhysRevC.67.014306 PACS number(s): 21.10.Hw, 23.40.Hc, 29.30.−h, 27.20.+n

I. INTRODUCTION

The radioactive nuclear beam facilities constructed during the past decade have enabled us to access nuclei far from the stability line. The observed exotic features, such as the neutron halo, the anomaly in the single-particle energy, and the change of the magic number, have been stringent tests for our understanding of the structure of nuclei, established so far for nuclei close to the stability line. It is now necessary to investigate more details of the structure of exotic nuclei over a wide region of the nuclear chart.

Determining the ground-state properties of nuclei, such as the mass, half-life, spin and parity, and electromagnetic moments, is the first step in understanding the nuclear structure. For a precise determination of the wave functions, also important is spectroscopic information associated with the excited states. Due to a large mass difference between the parent and daughter nuclei in a region far from the stability line, the β-decay process preferentially proceeds to the particle unbound states (typical excitation energy up to 10−20 MeV) in the daughter nucleus. A schematic example of an energy diagram is shown in Fig. 1 for the case of a neutron-rich nucleus. The discreteness of the decaying particle (or γ-ray) energy allows us to individually determine the excitation energy and the decay width of the excited states in the daughter nucleus, if we detect the decaying particle(s) or γ rays in coincidence with the β-rays. This is the typical method of β-delayed spectroscopy. One example involves the work by Harkewicz *et al.* [1] for ^{15}B. They determined the energy of the excited states and the Gamow-Teller transition strength $[B(\mathrm{GT})]$ for five excited states in ^{15}C above the neutron threshold. In addition to this information, the spin parities of the excited states are also important, since the sequence and position of excited states are essential to determine the nucleon-nucleon interactions and/or the nuclear structure. From the log ft values, the nature of the allowed transitions is assured, which constrains the spin parities to be $I_f=I_i-1$ or I_i or I_i+1, and $\pi_f=\pi_i$, where $I_i^{\pi_i}$ and $I_f^{\pi_f}$ are the spin parities of the initial and final states, respectively. However, these assignments are not unique and, apparently, not sufficient.

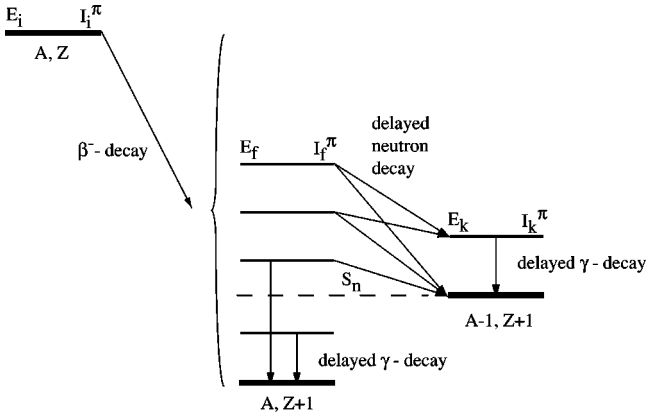

FIG. 1. Schematic diagram of β-delayed neutron decay.

*Electronic address: hiroari.miyatake@kek.jp

Another possible method is to make use of any β-decay anisotropy for the allowed transitions with respect to the orientation of the parent nucleus spin. Even if the parent nuclear spin is not oriented, if we observe the β rays in some direction we can constrain the spin orientation of the daughter nucleus; also, the γ rays which are subsequently emitted are circularly polarized. Therefore, if the γ-ray circular polarization is measured, unique spin-parity assignments can be made. This method is unfortunately not efficient for nuclei far from stability, because the measurements are limited to those states below the particle threshold, where the decay widths are often small, and the detection efficiency of the γ-ray polarimeter is also generally small.

Here we propose another method to assign the spin parity of excited states. We take advantage of the anisotropic β decay of a *spin-polarized* nucleus. By detecting the β-decay asymmetry in coincidence with delayed particle(s) or γ ray(s), we can determine the AP values for individual states, where A is the β-decay asymmetry parameter and P is the spin polarization of the parent nucleus. The asymmetry parameter (A) takes largely scattered discrete values, depending on the initial- and final-state spins, whereas the polarization (P), which is related to the reaction mechanism in producing the parent nucleus, is common for all β-decay transitions. It is therefore possible to determine the spins of states in the daughter nucleus as follows.

If the initial spin (I_i) and one of the final spins (I_f) are known, the polarization (P) can be evaluated from the AP value of the relevant transition. Then, other unknown I_f's become known. This method can be extended to a more general case where none of the final-state spins is known. The assignment can be done by searching for the least variance of P among the possible combinations of the I_f's. The feasibility of this method has been successfully tested for the β-delayed neutron decay spectroscopy of $^{15}\mathrm{B}_{\mathrm{g.s.}}$ ($I_i^\pi = 3/2^-$, $T_{1/2} = 10.5$ ms, $Q_\beta = 19.094$ MeV).

This paper is organized as follows. In Sec. II, we describe the principle of the method. In Secs. III and IV, we give details concerning the experiment and a data analysis. In Sec. V we discuss the scope of this method. Finally, in Sec. VI, we summarize the results and present some conclusions.

II. PRINCIPLE OF THE METHOD

Since β decay is a parity nonconserving process, β rays are emitted anisotropically with respect to the spin orientation of the parent nucleus. For the allowed transitions, the β-ray intensity [$W(\theta)$] is expressed as a function of the emission angle (θ) from the polarization axis as

$$W(\theta) \propto 1 + (v/c) AP \cos\theta, \tag{1}$$

where v, c, A, and P are the velocity of the β ray, the light velocity, the asymmetry parameter of the β transition, and the polarization of the parent nucleus, respectively. In the case of a large Q_β value, we can approximate that $v/c \sim 1$. The polarization (P) is a quantity associated only with the initial state, i.e., the ground state of the parent nucleus. On the other hand, the asymmetry parameter (A) is related to the spins of both the initial (I_i) and final states (I_f). For the allowed transitions, the spins of the final states are restricted to $I_f = I_i - 1$ or I_i or $I_i + 1$, and the parities must be the same: $\pi_f = \pi_i$. For these three spin states, the asymmetry parameters are expressed as follows:

$$A(I_i, I_f) = \begin{cases} \pm 1 & \text{for} \quad I_f = I_i - 1 \\ \dfrac{\pm 1/(I_i+1) - 2r\sqrt{I_i/(I_i+1)}}{1+r^2} & \text{for} \quad I_f = I_i \\ \mp \dfrac{I_i}{I_i+1} & \text{for} \quad I_f = I_i + 1. \end{cases} \tag{2}$$

The upper (lower) sign is applicable for the β^+ (β^-) transition. Here, r in the middle case is the mixing ratio of the Fermi to the Gamow-Teller transition probabilities, $r = C_V\langle 1\rangle / C_A\langle\sigma\rangle$. The asymmetry parameter varies to a large extent according to the final state spin (I_f). In the $^{15}\mathrm{B}_{\mathrm{g.s.}}$ ($I_i^\pi = 3/2^-$) case, the possible I_f^π is either $1/2^-$ or $3/2^-$ or $5/2^-$, and the asymmetry parameter (A) is, respectively, either -1.0 or -0.4 or $+0.6$. Here, in the middle case, a pure Gamow-Teller transition is assumed, as is reasonably done for most of the neutron-rich nuclei.

If β-delayed particles and/or γ rays are measured in coincidence with the β-ray asymmetry, we can determine the AP values in Eq. (1) for each transition. It is to be noted here that the polarization (P) is common for all transitions. As a result, if the initial-state spin (I_i) and one of the final-state spins (I_f) are known, we can evaluate P, and can then determine the A's for any spin-unknown states. The discreteness of the A value enables unambiguous spin assignments (method I).

Let us consider a more general case (method II) where we know I_i, and none of the final state spins (I_f). We cannot determine P naively. There are three candidate values of A for each transition. In the case of ^{15}B, we observed five allowed transitions leading to neutron-emitting states, as Harkewicz *et al.* [1]. Therefore, there are 243 ($=3^5$) combinations of possible A's. For each allocated A_j value (j is used to denote the transitions, $j = 1,2,\ldots,5$), the polarization is evaluated as $P_j = (AP)_j / A_j$, where $(AP)_j$ is the measured asymmetry. For the proper combination of A, i.e., the correct spin assignments for all five final states, the evaluated P_j's should be consistent with each other. It is therefore expected that for improper combinations of A, the expected value of P should have systematic errors, and the variance of P should become larger. In other words, the correct assignment should give the least variance of P. This is the *guiding principle* to determine I_f's simultaneously.

For the ith set of A_j's, the mean polarization ($\overline{P_i}$) is calculated as

$$\overline{P_i} = \frac{\sum_j P_j w_j}{\sum_j w_j} \quad (i = 1,2,\ldots,243), \tag{3}$$

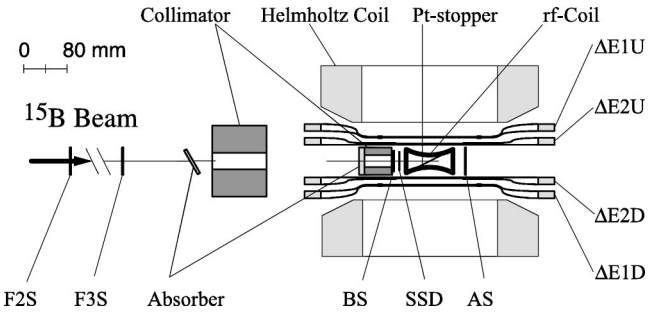

FIG. 2. Cross-sectional view of the β-NMR apparatus.

where w_j is the statistical weight factor for each P_j value,

$$w_j = \frac{A_j^2}{\sigma^2_{(AP)_j}}, \tag{4}$$

with the experimental error $\sigma_{(AP)_j}$ for $(AP)_j$. By definition, the reduced χ^2_ν for the ith set is given as

$$\chi^2_\nu(\overline{P}_i) = \frac{1}{\nu}\sum_j (P_j - \overline{P}_i)^2 w_j \quad (i = 1,2,\ldots,243), \tag{5}$$

where ν indicates the degree of freedom ($\nu = 4$ in this case). The above-mentioned guiding principle is that the most probable combination of A_j should give the *least* χ^2_ν among the 243 values for all possible combinations of A_j. In that case, $\overline{P}_i$ can be regarded as the statistically expected value of P.

III. EXPERIMENTAL PROCEDURE

The feasibility of the present method has been experimentally tested for the β-delayed neutron decay of spin-polarized^{15}B.

A. Spin-polarized ^{15}B

A radioactive nuclear beam of ^{15}B was produced in the projectile-fragmentation reaction of a 110-MeV/nucleon ^{22}Ne beam from the RIKEN ring cyclotron on a ^{9}Be target (832 mg/cm^2). For calibrating the neutron counters, a ^{17}N beam was also produced in the same beam-target combination. The spin polarization of ^{15}B was produced by taking advantage of the reaction mechanism, following a method by Asahi and co-workers [3,4]: The ^{15}B fragments emitted at a finite angle of $\theta_{\rm lab} = 2.0° \pm 1.0°$ ($\Delta\phi = \pm 1.0°$) were accepted by the fragment separator RIPS [5] and isotopically separated. The direction of the polarization was perpendicular to the reaction plane, which was the same as the median plane of the separator. ^{15}B fragments with momentum $p = 6.096 \pm 0.183$ GeV/c ($\Delta p/p = \pm 3\%$) were transported to the mass-dispersive focal plane (F2), where isotope selection was made. As shown in Fig. 2, a thin plastic scintillator (F2S; 2 mm thick) and a Si detector (500 μm) were placed at F2 to identify ^{15}B by taking advantage of the ΔE-TOF (time of flight) correlation. An F2S scintillator was also used as one of the trigger signals for the data-taking system. The ^{15}B beam was then focused and implanted into a Pt foil (100 μm thick) placed at the final focus point (F3), which was located 1.5 m downstream of F2. The β-ray asymmetry was measured by the β-NMR system surrounding the Pt foil, as shown in Fig. 2. In order to monitor the ^{15}B beam and to make sure of its implantation into the Pt foil, three plastic scintillators and a Si detector were placed upstream (F3S, BS, and SSD) and downstream (AS) of the Pt foil. The thicknesses of the detectors were 1 mm (F3S), 2 mm (BS), 500 μm (SSD) and 2 mm (AS). To adjust the implantation depth of the ^{15}B beam in the Pt foil, an Al energy absorber was inserted between the F3S and BS scintillators. The absorber thickness was adjusted by tilting it. The trigger condition was $(\Delta E1U \cap \overline{\Delta E1D} \cap \Delta E2D) \cup (\Delta E1D \cap \overline{\Delta E1U} \cap \overline{\Delta E2U})$. This prevented cosmic-ray events. Although the beam contaminant ^{3}H and ^{6}He were observed at F2 with a similar amount to ^{15}B, their effects were negligible in the β-neutron coincidence events, as confirmed in the β-decay time spectrum.

B. β-NMR system

The β-ray asymmetry was precisely measured using the β-NMR technique [6]. The principle is briefly described in the following. According to Eq. (1) the β-ray counts are most asymmetric in the directions parallel ($\theta = 0$) and antiparallel ($\theta = \pi$) to the polarization axis, as expressed by

$$\begin{aligned} N_0(I_i,I_f) &\propto \varepsilon_0^\beta \varepsilon^n (1 + A(I_i,I_f)P), \\ N_\pi(I_i,I_f) &\propto \varepsilon_\pi^\beta \varepsilon^n (1 - A(I_i,I_f)P), \end{aligned} \tag{6}$$

where $N_\theta(I_i,I_f)$ are the β-ray counts in the direction θ coincident with the delayed neutrons from a specific excited state in ^{15}C(I_f), and ε_π^β and ε^n are the detection efficiencies for β-rays and neutrons, respectively. Thus the product $A(I_i,I_f)P$ can be deduced as

$$A(I_i,I_f)P = \frac{N_0(I_i,I_f)\varepsilon_\pi^\beta - N_\pi(I_i,I_f)\varepsilon_0^\beta}{N_0(I_i,I_f)\varepsilon_\pi^\beta + N_\pi(I_i,I_f)\varepsilon_0^\beta}. \tag{7}$$

Although the neutron counter efficiency (ε^n) is canceled out here, $A(I_i,I_f)P$ is subject to the asymmetry in the β-ray counter efficiencies ε_0^β and ε_π^β. We therefore rotated the spin orientation by 180 degrees by taking advantage of the adiabatic fast passage (AFP) method in nuclear magnetic resonance (NMR). By using the β-ray counts ($N^*_\theta(I_i,I_f)$) when the nuclear spin is rotated by 180°, $A(I_i,I_f)P$ is obtained freely from the spurious asymmetries

$$\begin{aligned} A(I_i,I_f)P &= \frac{\sqrt{R}-1}{\sqrt{R}+1}, \\ R &= \frac{N_0(I_i,I_f)/N_\pi(I_i,I_f)}{N^*_0(I_i,I_f)/N^*_\pi(I_i,I_f)}. \end{aligned} \tag{8}$$

In the present work, β-ray counter telescopes were set above and below the Pt stopper, as shown in Fig. 2. Each

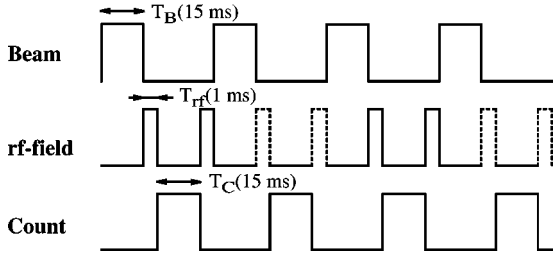

FIG. 3. Time sequence of the beam irradiation (T_B), rf-field application for AFP (T_{rf}), and β-n counting (T_C). A rf-field was not applied in the period expressed by the dotted line.

telescope consisted of two plastic scintillators (2 mm and 5 mm thick), and the light output from each scintillator was detected by two small photomultiplier tubes (PMT, HAMAMATSU R5600P) in coincidence. This type of PMT functioned well even under the magnetic field, as discussed below. The solid angle of each telescope was 29% of 4π, giving almost the largest figure of merit, $(\text{polarization})^2 \times (\text{yields})$. The finite solid angle causes spuriously smaller AP values, approximately 70% of that estimated by Eq. (8), where an infinitesimally small solid angle is assumed. The reduction was imposed not on A, but on P, since A is solely determined by the β-transition. A pair of Helmholtz coils was set in the direction of polarization, i.e., perpendicular to the median plane of the RIPS, to apply a static magnetic field (500.0 G) on the region of the stopper (see Fig. 2). This field served not only as that for the magnetic resonance, but also as a holding field to preserve the spin polarization. The spin-relaxation time of ^{15}B in Pt is known to be much longer than its lifetime [6]. For the AFP operation, an rf-magnetic field was applied in the direction perpendicular to the static field by a pair of saddle-shaped coils. This shape was designed so that the decay neutrons would not be disturbed by the coils. The same care was taken for designing the supports for the foil and scintillators. An rf-magnetic field was swept linearly from low to high frequency around the resonance frequency of $\nu_0 = 676$ kHz [4]. The primary ^{22}Ne beam was pulsed with a 15 ms on-beam period and a 17 ms off-beam period. In order to induce the AFP process in every other off-beam period, the rf-field was applied during 1 ms at the very beginning and the very end of the off-beam period. Between the rf-application periods the β rays and neutrons were detected, as schematically shown in Fig. 3.

C. Neutron counters

The β-delayed neutrons from ^{15}C* were detected by plastic scintillation counters surrounding the β-NMR system, as shown in Fig. 4. The neutron counters were set so as to detect neutrons emitted vertically to the β-ray direction. This geometry minimized the neutron energy broadening due to the β-ray recoil effects. The neutron energies were determined through the time-of-flight (TOF), referred to the β-ray signal as the start pulse. The plastic scintillator (BICRON BC408) was curved in the vertical direction with a 150 cm radius (160-cm arc length) and a 40-cm latitudinal width in the median plane. The neutron energy resolution was estimated to be 30 keV (full width at half maximum) for 1-MeV neutrons, which was primarily determined by the scintillator thickness (2.0 cm).

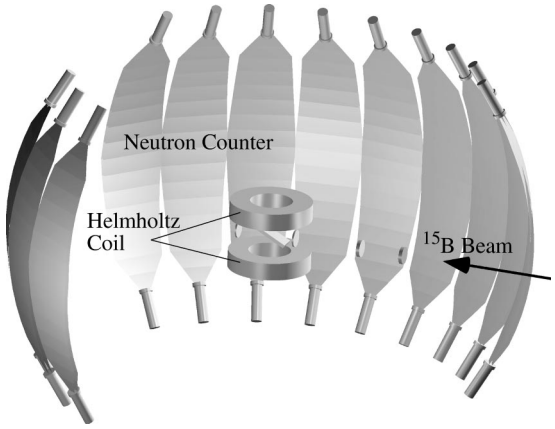

FIG. 4. Neutron counters. The β-NMR system shown in Fig. 2 is placed at the center of the counter array.

Twelve of such scintillators were placed 150 cm away from the Pt stopper. The scintillators altogether covered a 21.1% solid angle of 4π. In order to achieve a high neutron detection efficiency, the scintillator geometry was carefully designed with respect to light reflection and attenuation, and two photomultiplier tubes (HAMAMATSU H1161) were directly attached to the scintillator on both ends of the longitudinal arc. As a result, we could lower the threshold down to 3.4(27) keV_{ee} (electron equivalent energy) and, consequently, a high efficiency of 0.47% (5.6% with 12 scintillators) was achieved for 1-MeV neutrons. In order to get rid of any time fluctuation due to neutron hit positions along the arc, the mean value of two time to digital converter (TDC) data from PMT's was used. The pulse-height information (Q) from PMT's was also recorded to correct for any time slewing, i.e., the time jitter of leading-edge discriminators depending on the pulse height (Q). The slewing correction was successfully made by assuming the relation

$$t = t_0 - \sigma\sqrt{2\ln(Q/Q_{th})}, \tag{9}$$

with the threshold $Q_{th} = 3.4$ keV_{ee} and the signal rise time $\sigma = 2.2$ ns. The former value was determined from an efficiency calibration measurement (discussed later), and the latter was evaluated from the best slewing correction. The latter is consistent with a typical specification value of 2.3 ns [7]. Those β-n coincidence events with more than one neutron counter were rejected to reduce the background from cosmic rays and neutron scattering.

IV. RESULTS

A. Calibration of neutron counters with ^{17}N beam

For a precise determination of A, it is necessary to identify and decompose the peaks in the TOF spectrum and to precisely evaluate the neutron counts associated with each peak. In general, the peaks overlap with each other due to the effects discussed below. Therefore, it is important to achieve precise peak decomposition with accurate response functions

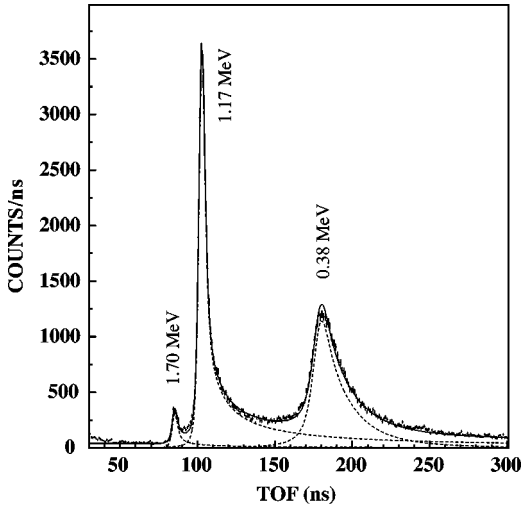

FIG. 5. TOF spectrum of β-delayed neutrons from ^{17}N. The energies are given in E_n. The fitting results are shown by lines. The dashed lines show the components attributed to each transition and the solid line shows their sum.

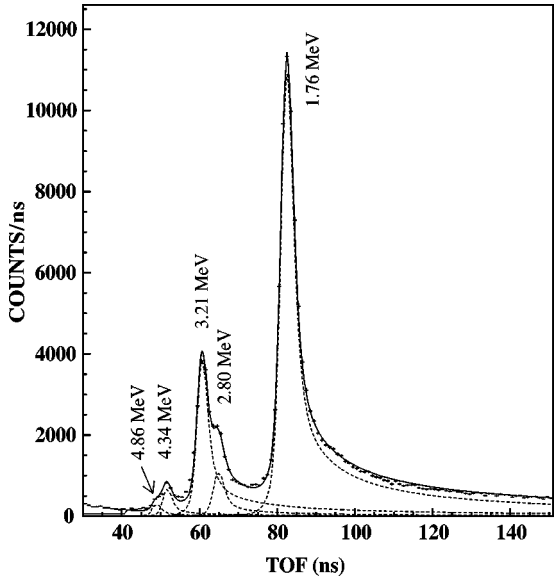

FIG. 6. TOF spectrum of β-delayed neutrons from ^{15}B. The fitting results are shown by lines. The dashed lines show the components attributed to each transition and the solid line shows their sum.

of the neutron counter. In order to obtain the response functions, β-delayed neutrons from ^{17}N were measured. The decay property of $^{17}N_{g.s.}$ ($I^{\pi}=1/2^{-}$, $T_{1/2}=4.17$ s, and $Q_{\beta}=8.680$ MeV) is well established [8]. Figure 5 shows the result. The neutron counts are plotted as a function of the flight time. Three peaks can be clearly seen. It can also be noticed that each peak has a long tail on the lower-energy side. This spectrum was fitted by analytic functions which took into account the following effects.

(a) The level width of the initial state of neutron decay (^{17}O* in the above case). For this, a Lorentz form function as the flight time (t) was assumed,

$$H(t)=K\frac{\Gamma/2\pi}{\left[\frac{m}{2}\left(\frac{L}{t}\right)^2-E_n\right]^2+(\Gamma/2)^2}\left|\frac{\partial E_n}{\partial t}\right|, \qquad (10)$$

where K, m, E_n, Γ, L are the amplitude, the neutron mass, its kinetic energy, the level width, and the flight length, respectively. The factor $|\partial E_n/\partial t|=mL^2/t^3$ is for the conversion from E_n to t.

(b) The uncertainty in L due to the scintillator thickness, the counter misalignment, the finite beam-spot size (12×13 mm^2 in $x\times y$), and so on. These effects were incorporated by a Gaussian with the standard deviation (σ_t), which is expressed by the mean flight length (L) and its deviation (σ_L), $\sigma_t=t\times\sigma_L/L$.

(c) The effects of the neutron scattering by material around the stopper, such as Helmholtz coils, before neutrons reach the scintillator. This causes a tail in the larger t side (lower E_n side) of the peak. To incorporate the effect, an empirical function converting from an unscattered spectrum with flight time (t) to the scattered one with flight time (t'),

$$f(t,t')=\frac{a}{t'-(t-b)} \quad (t\leqslant t'),$$

$$f(t,t')=0 \quad (t>t'), \qquad (11)$$

was assumed with the parameters a and b. It was found that the parameters showed a negligibly small neutron-energy dependence. Therefore, they were fixed for all neutron peaks.

(d) The intrinsic time resolution of the scintillator and/or PMT of both the β ray and the neutron counters and of the associated electronics circuits. A Gaussian was assumed for the overall effects, and the constant width parameter was determined to be $\sigma_t'=0.75(4)$ nsec by fitting the γ-ray peak, which is not shown in Fig. 5.

(e) The constant background due to accidental coincidence between the β-counter events and background events in the neutron counters.

(f) The background due to β-ray scattering before reaching the β-ray telescope. This effect gives a monotone decreasing spectrum with t (TOF).

In the fitting procedure, first of all, the absolute time scale was calibrated by referring to the peaks in Fig. 5. However, presumably because the neutron energy (E_n) is limited below 1.7 MeV there, the evaluated E_n's for peaks in the ^{15}B data (Fig. 6) were slightly higher ($\sim2\%$) in the region $E_n>3$ MeV than those calculated from the Ajzenberg's energy level compilation for ^{15}C [2]. Therefore, the time calibration was again made by adopting neutron energies both from the ^{17}N data [8] and the ^{15}B data [2], and the flight length uncertainty was determined by fitting the high energy side of the 1.17-MeV peak in Fig. 5 with a convoluted function incorporating the effects of (a), (b), and (d). The best-fit values were $L=149.52(1)$ cm and $\sigma_L=1.81(5)$ cm. They are consistent with the designed values. The parameters a and b for the neutron-scattering effect (c) were determined so that $a=0.101(2)$ nsec and $b=5.1(4)$ nsec, by fitting the 1.17- and

TABLE I. Levels in ^{15}C observed in the present work: neutron energy, E_n; level energy, E_x; and width, Γ.

E_n (MeV)		E_x in ^{15}C (MeV)		Γ (keV)	
present work	estimated from Ref. [2]	present work	Ref. [2]	present work	Ref. [2]
→	1.759(4)	→	3.103(4)	26(7)	<40
→	2.802(3)	→	4.220(3)	37(10)	<14
→	3.210(8)	→	4.657(9)	50(13)	
→	4.338(8)	→	5.866(8)	12(3)	
4.861(8)	4.82(6)[a]	6.426(8) [b]	6.417(6)	14(4)[b]	~ 50

[a]Reference [1].

[b]These values were obtained under the assumption of a single neutron peak at 4.861 MeV.

1.70-MeV peaks in Fig. 5 with convoluted function incorporating the effects through (a) to (d) and background [(e) and (f)].

The fitted results are shown by the lines in Fig. 5. The dotted lines are the components attributed to each transition and the solid line is their sum. The reduced χ square of the overall fitting was 2.2. The absolute neutron detection efficiency was evaluated from the counts of the 1.17-MeV neutron peak in Fig. 5. The efficiency was compared with a simulation code by Cecil *et al.* [9]. It was found, as mentioned before, electron equivalent threshold $Q_{th} = 3.4$ keV$_{ee}$. In the following analyses of the ^{15}B data, parameters other than the amplitude and the level width (Γ) in Eq. (10) were fixed to those determined in the above fitting, and their errors were propagated to the fitting errors.

B. Neutron TOF spectrum with ^{15}B beam

With the spin-polarized ^{15}B, four kinds of TOF spectra were obtained with the β rays emitted upward or downward and spin-up or -down. The amplitude in Eq. (10) for each peak in the respective spectra are proportional to $N_0(I_i, I_f)$, $N_\pi(I_i, I_f)$, $N_0^*(I_i, I_f)$, and $N_\pi^*(I_i, I_f)$ in Eq. (8). In order to identify the peaks, a high-statistics spectrum was obtained by summing the four spectra, as shown in Fig. 6.

There are three major peaks and some peaks significantly overlap with each other. This situation is essentially the same as in the previous work by Harkewicz *et al.* [1]. As discussed above the intrinsic time resolution of the detector system is estimated to be ~ 360 keV at the 50–60-nsec region. Therefore, we assumed five isolated peaks which are apart from others more than 360 keV. These peaks were unambiguously assigned as being due to neutron decays from the known excited states in ^{15}C, except for the smallest peak at $t = 49$ ns ($E_n \sim 4.8$ MeV). For this peak, Harkewicz *et al.* [1] determined $E_n \sim 4.82(6)$ MeV, thus $E_x = 6.38(6)$ MeV, and pointed out that the peak was associated with the level in ^{15}C at 6.358(6) MeV or 6.417(6) MeV, or a mixture of them. It is also consistent with the 6.449(7)-MeV level [2]. Because of the indefinite information concerning of this peak, we regarded it as the peak associated with a single neutron transition and treated its energy as a free parameter in the fitting, and other E_n's were fixed to those in Ref. [2]. As a result, we determined a value different from that of Ref. [1], $E_n = 4.861(8)$ MeV, which corresponds to $E_x = 6.426(8)$ MeV. The small uncertainty is due to the well-established response function and small number of free parameters (K, and Γ for five peaks and E_n for the 4.86-MeV peak). The determined E_n is consistent with the state at 6.417(6) MeV, but with neither of the states at 6.358(6) nor 6.449(7) MeV [2]. However, because of the limited statistics (2400 counts) and the resolution (360 keV), it is not possible to exclude contributions from neutron decays of the 6.358(6)- and/or 6.449(7)-MeV states. Hereafter, we evaluate the AP value and assign the spin on the assumption of a single peak at $E_n = 4.86$ MeV. The results of the peak fitting are listed in Table I. The errors were estimated by the error propagation of statistical errors and systematic errors in the fitting procedure.

C. Spin assignments

The fitting was performed for the four TOF spectra independently of each other. The overall reduced χ_ν^2's were 2.4, 2.7, 2.6, and 2.5 for the spectrum of N_0, N_π, N_0^*, and N_π^*, respectively. The AP values were deduced for each neutron peak according to Eq. (8). The errors of the AP values were estimated by taking into account, in addition to the statistical errors, such errors as the systematic errors in the response functions discussed above, and the errors in the spectrum fitting. That is, the statistical errors of the neutron counts were multiplied by a scale factor, $\sqrt{\chi_\nu^2}$, where χ_ν^2 is the reduced χ square of the fitting in the respective TOF spectrum [10]. Table II summarizes the experimental AP values.

Harkewicz *et al.* [1] determined the log ft values for the five observed transitions. They were in the range 4.34–5.39. It is therefore concluded that all five states are associated with the allowed transitions, and that our I_f^π-assignment method can be applied to all of them.

1. Assignments with a known I_f^π: Method I

At first, let us assume that we know one of the final-state spin-parities in ^{15}C, together with the initial-state spin-parity, $I_i^\pi = 3/2^-$, of ^{15}B$_{g.s.}$. If we know that the $E_x = 3.103$ MeV state, which has the highest statistics, is $I_f^\pi = 1/2^-$ [2], we can determine the polarization as $P = -2.80(46)\%$, because the asymmetry parameter associated with this state is -1. The sign of the polarization is consistent with a kinematical consideration [3]. Thus, the experimental asymmetry parameters

TABLE II. Experimental AP values and spin-parity assignments.

E_x in ^{15}C	experimental AP	most probable A	spin-parity assignment	
			present work	Ref. [2]
3.103(4)	$+2.80(46)$	-1.0	$1/2^-$	$1/2^-$
4.220(3)	$-2.8(16)$	$+0.6$	$5/2^-$	$5/2^-$
4.657(9)	$+0.44(85)$	-0.4	$3/2^-$	$3/2^-$
5.866(8)	$+2.4(22)$	$[-1.0,-0.4]$	$[1/2^-,3/2^-]$	$1/2^-$
6.426(8)	$+5.2(35)$	-1.0	$[1/2^-]$	[3/2,5/2,7/2]

(A) for other states can be immediately evaluated as $A=+1.00(58),-0.16(31),-0.87(80)$, and $-1.9(13)$ for the states at $E_x=4.220$, 4.657, 5.866, and 6.426 MeV, respectively. Here, the error in the AP value of the 3.103-MeV state is propagated to the errors in the A values for other states. These experimental asymmetry parameters are plotted in Fig. 7. The horizontal lines in the figure indicate the possible values of A for allowed transitions from $^{15}\mathrm{B}_{\mathrm{g.s.}}$. It can be seen that the experimental A values of the 4.220-, 4.657-, and 6.426-MeV states are consistent with $A=+0.6,-0.4$, and -1, respectively, within those 1σ deviations. By adopting the A values determined here, the I_f^π's of these states are assigned to be $5/2^-$, $3/2^-$, and $1/2^-$, respectively. The spin-parity assignments for the former two states agree with the previous assignments [2].

No definite spin-parity assignment has been made so far for the 6.426-MeV state; only a suggestion has been made from the angular-distribution data of the $^{14}\mathrm{C}(d,p)^{15}\mathrm{C}$ reaction, i.e., I_f^π is to be either $3/2^+$, $5/2^+$, $5/2^-$ or $7/2^-$ [11]. However, the angular distribution has no crucial sensitivity to spin-parity. As mentioned before, the log ft value (5.39) for the transition leading to this state requires a minus parity. As can be seen in Fig. 7, it is most probable that $I_f^\pi=1/2^-$ for this state, which does not agree with any of the above suggestions.

The A value for the 5.866-MeV state is consistent both with $A=-0.4(I_f^\pi=1/2^-)$ and $-1(3/2^-)$ within the 1σ deviation, although this state is assigned as $1/2^-$ [2]. In order to exclude the incorrect assignment with higher probability, more statistics are needed for the 5.866-MeV data. This is discussed in Sec. V.

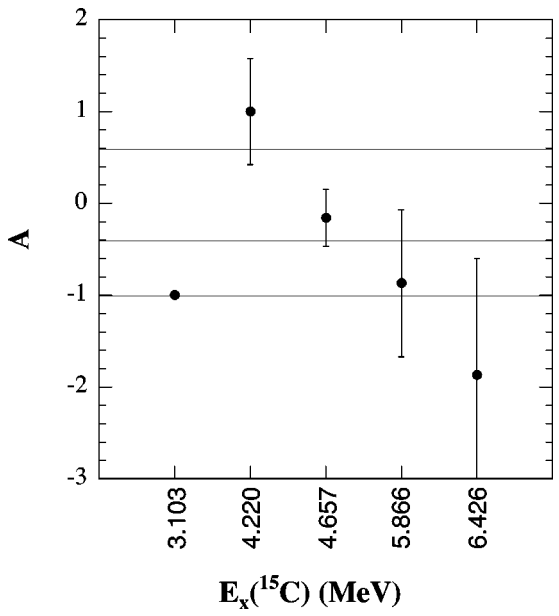

FIG. 7. Experimental asymmetry parameters for transitions leading to the states in ^{15}C when it is assumed that the 3.103-MeV state is $I_f^\pi=1/2^-$. The horizontal lines show the possible values of A for allowed transitions from $^{15}\mathrm{B}_{\mathrm{g.s.}}$. For $I_f^\pi=1/2^-$, $3/2^-$, and $5/2^-$, A should be -1, -0.4, and $+0.6$, respectively.

2. Assignments without known I_f^π: Method II

When none of the I_f^π's is known, the method of least variance of P should be applied. For all possible 243 combinations of I_f's, χ_ν^2 of Eq. (5) and the mean polarization ($\overline{P}$) of Eq. (3) were calculated. Their correlation is shown in Fig. 8. Although the χ_ν^2 values range widely from 0.4 to 9.9, the $\overline{P}$ values show a rather discrete feature: There are three groups with respect to the $\overline{P}$ value. This is explained by the discreteness of the A value, as follows. Because the 3.103-MeV state has the highest statistics, the mean polarization ($\overline{P}$) is significantly governed by P_j of the 3.103-MeV data. Among 243 data points, 81 give positive $\overline{P}$ values, where an incorrect value of $A=+0.6$ is allocated for the transition to the 3.103-MeV state, without any exception. This gives $P_j=+4.67\%$ associated with this transition. The positive po-

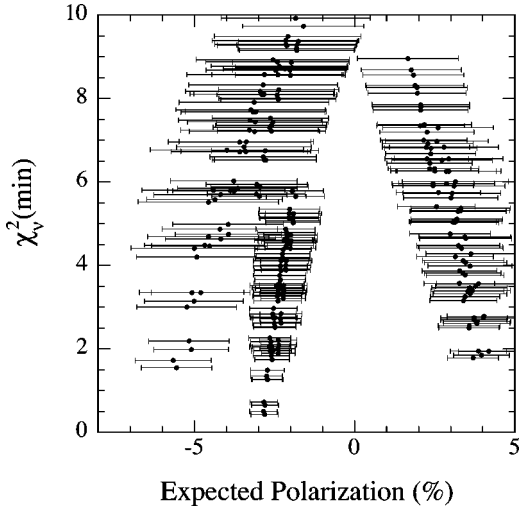

FIG. 8. χ_ν^2 as a function of the mean polarization ($\overline{P}$).

larization is unrealistic from the kinematical condition [3]. On the other hand, the data with a correct assignment of $A=-1$ for the 3.103-MeV state give almost stable $\overline{P}$, ranging from -1.9% to -2.8%. In the third group of the left side in Fig. 8, another incorrect value of $A=-0.4$ is allocated for the 3.103-MeV state.

As discussed before, the proper combination should be associated with the least χ^2_ν of P. It is achieved at $\chi^2_\nu=0.43$ and $\overline{P}=-2.81(42)\%$ with a A combination of $A=-1$, $+0.6,-0.4,-1$, and -1, for the 3.103-, 4.220-, 4.657-, 5.866-, and 6.426-MeV states, respectively. This combination gives the following set of I^π_f values: $1/2^-$, $5/2^-$, $3/2^-$, $1/2^-$, and $1/2^-$, respectively. It is to be noted that the former four assignments, including that for the 3.103-MeV state whose I^π_f value was assumed in method I, are consistent with the literature [2]. The second minimum χ^2_ν was obtained at $\chi^2_\nu=0.50$ and $\overline{P}=-2.84(43)\%$ with another I^π_f set where only the fourth assignment is different $[I^\pi_f(5.866)=3/2^-]$ from the least case. The third minimum χ^2_ν was obtained at $\chi^2_\nu=0.65$ and $\overline{P}=-2.80(42)\%$ with another A combination where only the fifth assignment is different from the least case: $I^\pi_f=1/2^-$, $5/2^-$, $3/2^-$, $1/2^-$, and $3/2^-$ for the 3.103-, 4.220-, 4.657-, 5.866-, and 6.426-MeV states, respectively. The mean polarization values $(\overline{P})$ for the three cases are consistent with each other and also with that by method I. Because of small difference of χ^2_ν values between the least (0.43) and the second minimum (0.50) cases, a unique assignment for the 5.866-MeV state is not possible also in method II. On the other hand, different assignments for the 6.426-MeV state cause rather large difference in the χ^2_ν values, and thus a unique assignment is possible, as in the case of method I, from the statistical analysis. Details of the statistical analysis are discussed in Sec. V.

V. DISCUSSION

A. Spin assignment for the 6.426-MeV state

A justification of the spin assignments can be made in terms of the χ-square test, as follows. We made the most probable spin assignment with a χ^2_ν value of 0.43 in method II. The significance of this assumption (assignment) is measured by the χ^2_ν value. In the case with a degree of freedom of $\nu=4$ (present case), a 70% level of significance corresponds to a reduced χ square $\chi^2_\nu=0.55$ [10]. This value is larger than the assumed χ^2_ν value. This means that the assumption is correct with the 30% confidence coefficient. However, another set of the spin assignments corresponding to the second χ-square minimum ($\chi^2_\nu=0.50$) cannot be excluded under this level of significance. On the other hand, the third minimum χ^2_ν case where only the 6.426-MeV state spin is differently assigned from the least χ^2_ν case, its χ^2_ν value (0.65) is larger than 0.55. Therefore, this assignment can be rejected under the 70% level of significance.

Another discussion can be made from the view point of the errors of polarization (P_j) evaluated from specific transition data $[(AP)_j]$. The P_j values should be consistent with the mean value $(\overline{P})$ which is determined by all transitions, if the respective assignment is properly made. Figure 9 shows the relative deviation of P_j $[(P_j-\overline{P})/\overline{P}]$ for the spin assignments with the least χ^2_ν (solid circle), the second (open circle), and the third (cross) minimum cases. All of the solid circles and open circles are consistent with zero within those 1σ deviations, whereas the cross for the 6.426-MeV state is out of this range. This fact implies that the third minimum assignment is highly improbable. It is noted again that above discussion is the based on the assumption, that the 4.8-MeV peak in the neutron spectrum would only be associted with a single neutron transition.

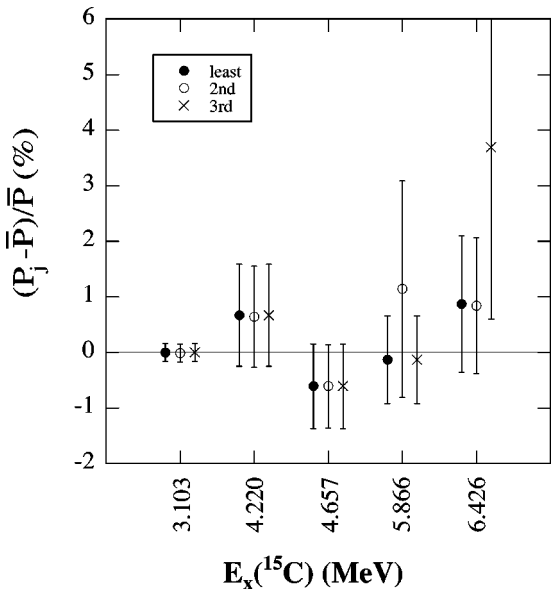

FIG. 9. Relative deviation of P_j $[(P_j-\overline{P})/\overline{P}]$ for spin assignments with the least χ^2_ν case (solid circles), with the second minimum case (open circles), and with the third minimum case (crosses).

B. Error consideration

The AP values may be affected by a systematic error, such as unstable polarization due to imperfect manipulation of the polarization and/or the beam. These errors contribute to enlarge all of the χ^2 values and do not affect any specific A combination. Therefore, the result of the present spin assignment is unchanged in a sense that the sequence of the χ^2 value does not change, although the fitting quality becomes worse because of the additional errors.

As displayed in Fig. 9, for unambiguous spin assignments, it is important that the errors of $(AP)_j$ due to statistics and peak fitting are smaller than the error in P_j due to an incorrect spin assignment. In the present work, the intense peak of the 3.103-MeV state gives an $\sim 10\%$ statistical error in $(AP)_j$, and the fitting error enlarges this by a factor of 1.6, resulting in an $\sim 16\%$ error of $(AP)_j$. On the other hand, an incorrect assignment causes a 60% error in P_j, which is by far larger than the former errors. This fact ensures the effectiveness of the present method. Actually, the 4.338-MeV peak to the 5.866-MeV state gives an $\sim 92\%$

error of $(AP)_j$ including an $\sim 58\%$ statistical error, which leads to the ambiguous spin assignment as mentioned above. In a general case where an incorrect assignment causes a smaller error than in the above case, it is important to reduce the statistical error. The relative statistical error of AP is expressed as

$$\frac{\delta(AP)}{|AP|} = \frac{1-(AP)^2}{4|AP|}\left(\frac{1}{N_0}+\frac{1}{N_\pi}+\frac{1}{N_0^*}+\frac{1}{N_\pi^*}\right)^{1/2} \sim \frac{1}{|AP|\sqrt{N}}, \tag{12}$$

where N is the total counts, $N=N_0+N_\pi+N_0^*+N_\pi^*$, and $|AP| \ll 1$ is assumed. The relative error depends more significantly on the $|AP|$ value than the total counts (N). For example, when $|AP|=2.4\%$ (the case of the 5.866-MeV state), the relative error, $\delta(AP)/|AP|=30\%$, requires the statistics of 2×10^4 counts for unambiguous spin assignment, which is about four times larger than the present statistics. While only 200 counts are required, if a ten-times larger polarization is achieved. It is to be noted that spin assignments in the present work have been performed with a rather small polarization of $P=-2.8\%$. The assignment can be done much more efficiently with highly polarized radioactive nuclear beams which have recently become available with state-of-the-art laser technologies [12].

VI. SUMMARY AND CONCLUSION

We propose a method of spin-parity assignments in the decay spectroscopy for a spin-polarized nucleus. It takes advantage of the discreteness of the β-decay asymmetry parameter (A), depending on the initial- and final-state spins. A feasibility test was performed for the β-delayed neutron decay of ^{15}B. The β-decay asymmetries were measured in coincidence with the delayed neutrons, and the AP values were evaluated for five allowed transitions leading to the excited states in ^{15}C. The peak analysis with well-established detector response function in the neutron TOF spectra enabled a precise determination of the level energies and the widths as E_x, $\Gamma=3.103(4)$ MeV, 26(7) keV; 4.220(3), 37(10); 4.657(9), 50(13); 5.866(8), 12(3); 6.426(8), 14(4). The level widths for these states were determined for the first time in the present work. The neutron peak for the last state has not been definitely analyzed, since the intrinsic energy resolution and the statistics were not enough to resolve the possible three states (6.358, 6.417, and 6.449 MeV).

From the AP values, the spin-parities were uniquely assigned as $I_f^\pi=1/2^-$, $5/2^-$, $3/2^-$, and $1/2^-$, respectively, for $E_x=3.103$-, 4.220-, 4.657-, and 6.426-MeV state. The assignments for the former three states are consistent with the previous assignments. The assignment $1/2^-$ for the 6.246-MeV state was suggested for the first time. Because of insufficient statistics for the 5.866-MeV state, an incorrect assignment $(3/2^-)$ could not be excluded, within the 1σ deviation from the correct one $(1/2^-)$. The present method is also applicable for β-delayed proton and α and γ decays. This method can be a powerful tool to investigate the exotic structures of nuclei far from stability.

ACKNOWLEDGMENTS

We would like to thank the entire staff of the RIKEN Ring Cyclotron, especially Dr. Y. Yano, for their encouragement throughout this work. This work was supported in part by Grant-in-Aids for Scientific Research of the Japan Ministry of Education, Science and Culture (Nos. 05452026 and 07640402).

[1] R. Harkewicz, D.J. Morrissey, B.A. Brown, J.A. Nolen, Jr., N.A. Orr, B.M. Sherrel, J.S. Winfield, and J.A. Winger, Phys. Rev. C **44**, 2365 (1991).
[2] F. Ajzenberg-Selove, Nucl. Phys. **A523**, 1 (1991).
[3] K. Asahi, M. Ishihara, N. Inabe, T. Ichihara, T. Kubo, M. Adachi, H. Takahashi, M. Kouguchi, M. Fukuda, D. Mikolas, D.J. Morrissey, D. Beaumel, T. Shimoda, H. Miyatake, and N. Takahashi, Phys. Lett. B **251**, 488 (1990).
[4] H. Okuno, K. Asahi, H. Ueno, H. Izumi, H. Sato, M. Adachi, T. Nakamura, T. Kubo, N. Inabe, A. Yoshida, N. Fukunishi, T. Shimoda, H. Miyatake, N. Takahashi, W.-D. Schmidt-Ott, and M. Ishihara, Phys. Lett. B **354**, 41 (1995).
[5] T. Kubo, M. Ishihara, N. Inabe, H. Kumagai, I. Tanihata, K. Yoshida, T. Nakamura, H. Okuno, S. Shimoura, and K. Asahi, Nucl. Instrum. Methods Phys. Res. B **70**, 309 (1992).
[6] K. Sugimoto, M. Ishihara, and N. Takahashi, in *Treatise on Heavy-Ion Science*, edited by D. A. Bromley (Plenum, New York, 1985), Vol. 3, pp. 395–536.
[7] Technical Data T-115 by Hamamatsu Photonics Ltd. (1987).
[8] H. Ohm, W. Rudolph, and K.-L. Kratz, Nucl. Phys. **A274**, 45 (1976).
[9] R.A. Cecil, B.D. Anderson, and R. Madey, Nucl. Instrum. Methods Phys. Res. **161**, 439 (1979).
[10] S. Brandt, *Statistical and Computational Methods in Data Analysis* (North-Holland, Amsterdam, 1970).
[11] J.D. Goss, P.J. Jolivette, C.P. Brown, S.E. Darden, H.R. Weller, and R.A. Blue, Phys. Rev. C **12**, 1730 (1975).
[12] C. D. P. Levy, R. Baartman, K. Jayamanna, R. Kiefl, T. Kuo, M. Olivo, G. W. Wight, D. Yuan, and A. N. Zelenski, in Proceedings of the 5th International Conference on Radioactive Nuclear Beams (RNB2000), Divonne, 2000 [Nucl. Phys. A (to be published)].